Development and Analysis of Electric Field Sensor Using $LiNbO_3$ Optical Modulator

Nobuo Kuwabara, *Member, IEEE,* Kimihiro Tajima, Ryuichi Kobayashi, and Fujio Amemiya

Abstract— **The sensitivity of an electromagnetic field sensor which uses a $LiNbO_3$ electrooptical crystal and an optical-fiber link is improved by employing a Mach–Zehnder interferometer, whose half-wave voltage is about 4 V at 1.3-μm wavelength, and a YAG laser pumped by a laser diode whose output power is 25 mW. The resulting frequency response is almost flat from 100 Hz to 300 MHz, and the minimum detectable electric field strengths are 0.22 mV/m at 50 MHz and 0.079 mV/m at 750 MHz. The variation of the sensitivity with the frequency and element length are analyzed using the moment method, and the calculated results agree with the measured results. The measurement of the cross-polarization of the sensor indicates that this property is similar to that of a dipole antenna. The improved sensor can measure an electromagnetic impulse whose peak value is larger than 10 V/m and whose width is wider than 5 ns.**

I. Introduction

Recent progress in electromagnetic compatibility (EMC) has created a need for a small wide-band electric field sensor for application in the electromagnetic interference (EMI) testing and design of information technology equipment as well as in the testing of EMI measurement facilities and the measurement of electromagnetic pulses. A serious problem for such sensors is the influence of the coaxial cable which connects the sensor to the level meter. Sensors which use resistive lines or an optical fiber in place of the coaxial cable have been developed to solve this problem.

The sensor that uses resistive lines, detects an electric field by means of a diode inserted between the dipole elements, and transmits the detected DC level to a voltmeter over the resistive lines. The sensor is so stable that it has been developed for use as a standard electric field sensor [1], [2]. However, it has the fundamental problem that it cannot measure frequency and phase information.

Therefore, sensors using an optical fiber have been developed. These sensors can be classified into two types: sensors that convert an electric-field strength to an optical signal by means of a laser diode or a light emitting diode [3]–[6] and those that convert an electric field strength to an optical signal by means of an optical modulator using electro-optical crystals such as $LiNbO_3$, $LiTaO_3$ [7]–[10].

The sensors using a laser diode have the advantage of increased sensitivity because of signal amplification in the sensor [6], but they also have the disadvantage of limited operation time due to battery capacity.

Manuscript received June 10, 1991; revised May 11, 1992.

The authors are with NTT Telecommunication Networks Laboratories 9-11 Midori-Cho 3-Chome Musashino-Shi, Tokyo 180 Japan.

IEEE Log Number 9202545.

The sensors that uses electrooptical crystals have the following superior points: the influence on electromagnetic fields is reduced because most of the sensor materials are nonmetallic, the operating time of the sensor is not limited, and the operating frequency bandwidth is very wide. Various sensors using bulk crystals, such as a 14-cm dipole electric filed probe [7] and an isotropic electric-field meter [8], have been proposed [7]–[9]. An electric field sensors using a Mach–Zehnder interferometer have been studied as a mean of increasing sensitivity [10], [11], but their sensitivity still needs to be improved because the minimum field strength that can be detected is only about 1.4 mV/m [10]. Furthermore, the frequency response of the sensor has not been clarified.

This paper describes a wide-band electric filed sensor, whose sensitivity is improved by using a low driving voltage optical modulator and a high-power light source. The sensor operates at 1.3-μm wavelength; a wavelength for which many optical components are being developed for telecommunication systems.

The sensitivity and frequency response are measured using a TEM cell. The sensitivity dependence on the frequency and on the element length of the sensor are analyzed using the moment method, and the results are compared with the measured values. The impulse response is also investigated by means of the TEM cell.

II. Configuration

The configuration of the sensor is illustrated in Fig. 1. Two metal rods are aligned, and they are separated by a small gap in which an optical modulator is located. When an electric field is applied to the metal rods, a voltage is induced across the gap. The optical modulator converts this voltage to an optical signal, and the electric field strength is obtained to measure this optical signal level by the photodetector.

Most of the sensor materials are nonmetallic to minimize the disturbance of the electric field. Metal-rod elements 50 mm long and 4 mm in diameter are connected to each electrode of the optical modulator, and the overall length of the sensor elements including the width of the modulator is 140 mm.

A 30 m-long polarization maintaining fiber connects the sensor to the optical source, and a 30-m-long single-mode fiber connects the sensor to the photodetector. This photodetector is a Ge avalanche photodiode (APD) operated by a constant voltage drive so as not to saturate the output voltage when the optical input power is high. The APD operation voltage is 38 V DC, the optical power input to the modulator is 11 dBm,

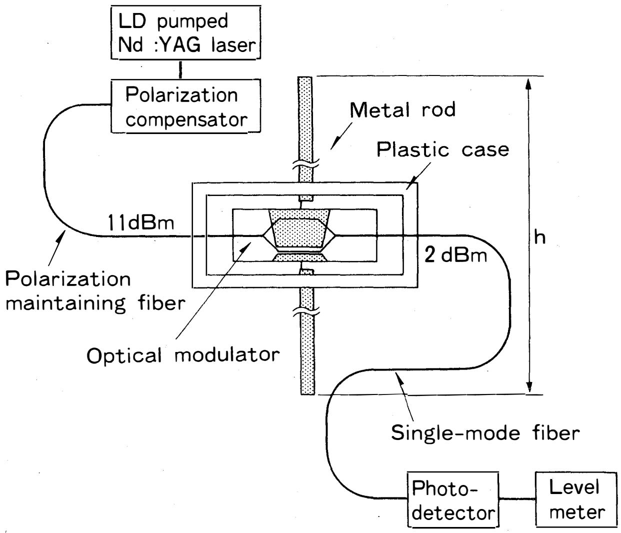

Fig. 1. Configuration of the proposed electric field sensor.

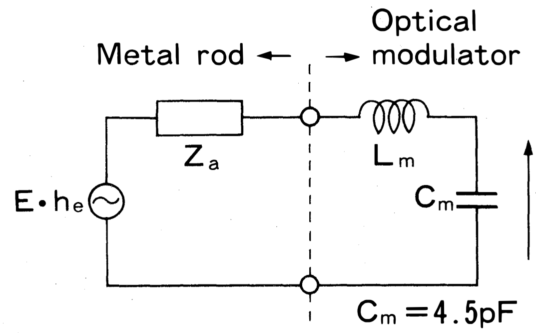

Fig. 2. Equivalent circuit of the sensor.

and the maximum optical power input to the photodetector is 2 dBm.

III. Improvement of Sensitivity

The electric field sensor shown in Fig. 1 can be represented by the equivalent circuit shown in Fig. 2, where C_m is the input impedance of the optical modulator, Z_a is the driving point impedance of the dipole element formed by the pair of metal rods [12], h_e is the effective length of the dipole element [12], and L_m is the inductance caused by the contact lead between the metal rods and the electrodes of the modulator. The input impedance C_m is usually represented by a capacitance because the terminal of the optical modulator is insulated. Using this equivalent circuit, the voltage applied to the optical modulator V_c is given by

$$V_c = E * h_e/(1 + \omega C_m(jZ_a - \omega L_m)) \quad (1)$$

where E is the electric field strength and ω is the angular frequency.

When a Mach–Zehnder optical modulator is used, the relation between the voltage applied to the optical modulator and the output voltage at the photodetector V_r is given by [13]

$$V_r = C_F * P_{\text{in}} * (1 + \cos(\pi V_C/V_\pi + \phi))/2 \quad (2)$$

where P_{in} is the optical input power of the modulator, C_F is a conversion factor that includes the efficiency of the photodetector, the insertion loss of the optical modulator and the optical fiber loss, ϕ is an optical bias angle caused the intrinsic phase difference between the interferometer arms, and V_π is the half-wave voltage of the optical modulator.

Substituting (1) into (2), the relation between the electric field strength and the output voltage is given by

$$\begin{aligned} V_r = {} & C_F * P_{\text{in}} \\ & * (1 + \cos(\pi * (E * h_e/(1 + \omega C_m(jZ_a - \omega L_m))) \\ & \div V_\pi + \phi))/2. \end{aligned} \quad (3$$

Equation (3) shows that a powerful optical source and low halfwave voltage optical modulator effectively improve sensitivity. Therefore, this sensor uses a wide-band and low driving power optical modulator whose half-wave voltage is about 4 V at 1.3 μm wavelength [13]. This modulator is a Mach–Zehnder interferometer formed from a 7- by 0.7-μm waveguide on a 10 mm by 40 mm Z-cut $LiNbO_3$ substrate. The electrode length is 27 mm and the gap width is 15 μm. This sensor also uses a high power Nd:YAG laser pumped by a laser diode as a light source. The output power of the laser is 25 mW and the oscillation wavelength is 1.3 μm. The optical power is 11 dBm at the modulator is obtained.

If the RF voltage V_c is small, the optical power is the maximum at an optical bias angle of 0°, but the RF signal at the fundamental frequency is zero in this bias. The bias angle should therefore be tuned to 90° to get the best signal response. It is difficult to tune the optical bias during the process of forming interferometer, so the interferometer whose optical bias angle is nearly 90° is selected from the formed several interferometers. Certainly the V_π for the modulator changes between the TE and TM mode of the propagation in the waveguide. A 1 kHz and 15 V peak-to-peak triangular wave was applied between the metal rods, and the polarization compensator was tuned to get a low half-wave voltage and the best signal response.

IV. Frequency Response and Sensitivity

The frequency response and sensitivity of this sensor were measured by using a 900 mm by 300 mm by 300 mm transverse electromagnetic (TEM) cell whose bandwidth was tuned to 800 MHz by absorbers. A signal from 35 to -100 dBm was supplied to the TEM cell, and its power was measured by a power meter or level meter connected to the output terminal of the cell. An electric field of from 7.9×10^1 V/m to 1.4×10^{-5} V/m was generated in the TEM cell, and the output level of the photodetector was measured by a level meter whose bandwidth was 7.5 kHz.

The relation between the optical input power of the sensor and output level of the photodetector is shown in Fig. 3, where the output levels of the photodetector are normalized by the maximum value. The optical input power is tuned by an optical attenuator, and at frequency of 50 MHz and field strength of 0.64 V/m are selected for the experimental

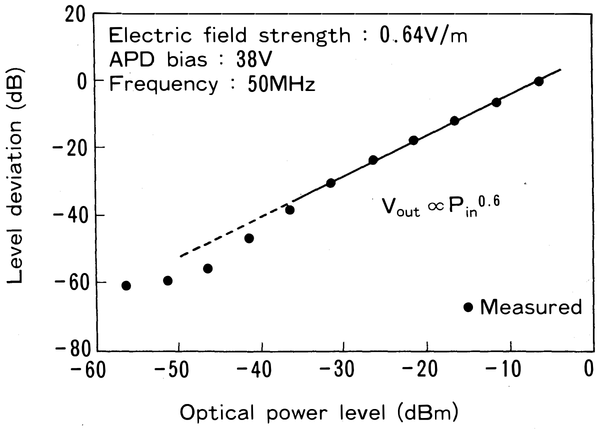

Fig. 3. Sensitivity dependence on optical power of the sensor.

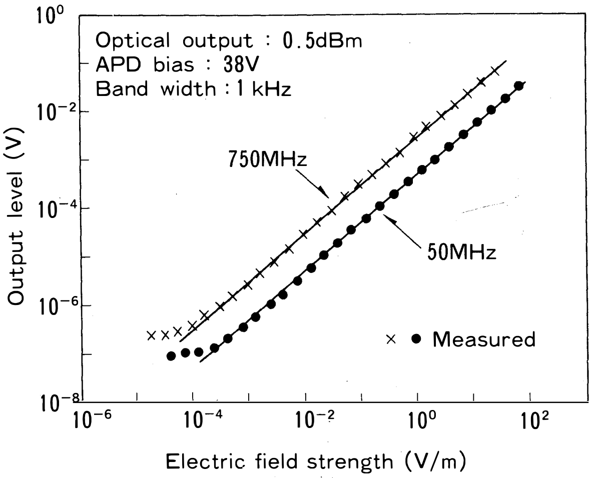

Fig. 4. Sensitivity of the sensor.

conditions. The measured results show that the output voltage increases proportionally with the optical power. This means that a high-power optical source improves the sensitivity of the sensor.

The sensitivity of the sensor is shown in Fig. 4. The applied electric field strength was calculated from the output level and the dimensions of the TEM cell, and the output voltage of the photodetector was measured with a level meter at 50 MHz and at 750 MHz. The 50 MHz frequency was selected because its response is flat, and the 750 MHz frequency was selected because the sensor exhibits maximum sensitivity at this frequency. The bandwidth of the level meter was set to 1 kHz. As shown in Fig. 4, the sensor exhibits an ideal linear response from 3.2×10^{-4} V/m up to 3.2×10^{1} V/m, and it has a dynamic range of 100 dB. Furthermore, for the data plotted in Fig. 4, the relation between output voltage and electric field strength can be written as

$$V_r(\mathrm{V}) = A_f \times E(\mathrm{V/m}) \tag{4}$$

where A_f is a transfer coefficient. Values for A_f of 4.5×10^{-4} (V/(V/m)) at 50 MHz and 3.2×10^{-3} (V/(V/m)) at 750 MHz are obtained from Fig. 4. Since the noise level of the photodetector is 1.0×10^{-7} V at 50 MHz and 2.5×10^{-7} V at 750 MHz, the minimum field strength that can be detected is 2.2×10^{-4} V/m (0.22 mV/m) at 50 MHz and 7.9×10^{-5} V/m (0.079 mV/m) at 750 MHz. The sensitivity of the reported sensor was 1.4 mV/m [10], so the sensitivity of the sensor is improved more than 25 dB.

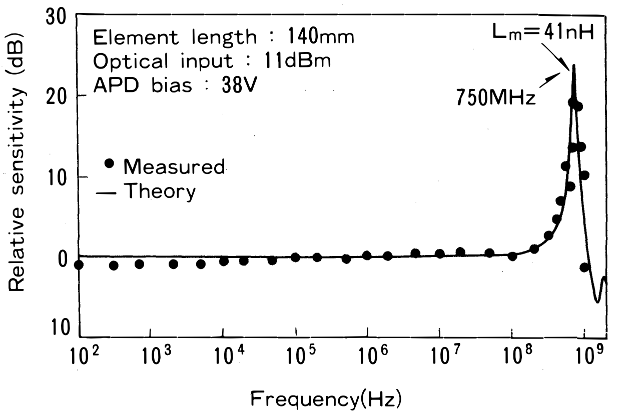

Fig. 5. Frequency response of the sensor.

The frequency response of the sensitivity was measured using the TEM cell. For these measurements, an electric field was applied to the sensor from 100 Hz to 1 GHz, and the output level of the photodetector was measured by the level meter. The electric field strength was calculated from the output level and the dimensions of the TEM cell. The relation between the photodetector output level and the applied electric field strength was measured. The results is shown in Fig. 5 where the plotted sensitivity is normalized to the value at 100 Hz. The relative sensitivity is almost flat from 100 Hz to 300 MHz, and it goes up above 300 MHz. The maximum sensitivity is obtained at about 750 MHz.

V. Theoretical Analysis of the Sensor

A. Theoretical Analysis

The sensitivity of the sensor goes up above 300 MHz as shown in Fig. 5. Since the frequency response of the optical modulator is almost flat from DC to 1 GHz [13], the frequency response is determined by the dipole element of the sensor and the contact lead between the dipole element and the electrode of the modulator. Therefore, the frequency response of the sensor was investigated by analyzing the equivalent circuit shown in Fig. 2.

The dipole element of the sensor is equivalent to that of a dipole antenna. The effective length and the driving point impedance can be calculated by the method of moment [14], [15]. If the dipole element is divided into segments of length Δz and the current on the element is expanded into a series of basis functions, the effective length and the driving point impedance are given by [12]

$$h_e = \sum_{n=1}^{M} \{I_n \cdot \Delta z / I_{(M+1)/2}\} \tag{5}$$

and

$$Z_a = V_{(M+1)/2} / I_{(M+1)/2} \tag{6}$$

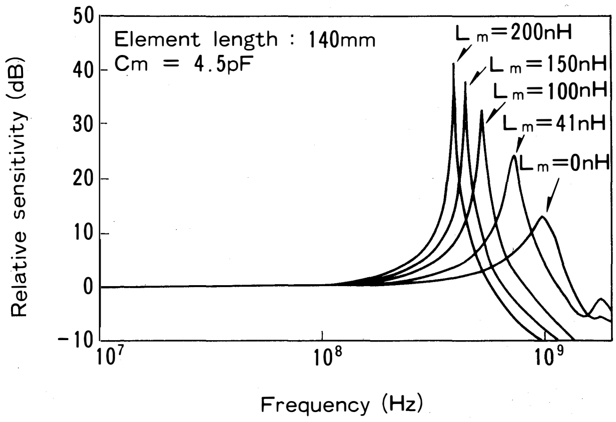

Fig. 6. Calculated frequency response of the sensor.

where I_n is the current in each segment, M is a number of segments, and $V_{(M+1)/2}$ and $I_{(M+1)/2}$ are respectively the segment voltage and current at the driving point of the dipole element.

In this analysis, a piece-wise sinusoidal function [15] was used as the basis functions, and I_n was calculated by mean of the method of moment [14]. Standard numerical integral formulas [15] were used in this calculation.

The value of the input impedance of the optical modulator C_m, 4.5 pF, is obtained by measuring the capacitance between the electrodes at 1 kHz.

B. Calculation and Results

The relation between the input voltage and optical modulator V_C and the electric field E was calculated based on the equivalent circuit in Fig. 2. Since the sensitivity of the optical modulator is almost flat from DC to 1 GHz [13], this calculation gives the frequency response of the sensor. The calculated results are shown in Fig. 6, where the inductance of the lead wire is changed from 0 to 200 nH. As shown in Fig. 6, the sensitivity of the sensor increases in proportion to the increase in inductance. On the other hand, the frequency at which sensitivity is the maximum decreases in proportion to the increase in inductance.

When L_m is 0 nH, the sensitivity is also increased at 1 GHz. This sensitivity increase is probably caused only by the increase in effective length. When L_m is larger than 0 nH, the sensitivity increase is caused by the resonance in the lead-wire inductance as well as the increase in the effective length.

The L_m of 41 nH is obtained to fit the maximum sensitive frequency in Fig. 6 to the measured results shown in Fig. 5, and the calculated values are shown by the line in Fig. 5. The figure shows that the calculation results at L_m of 41 nH almost agree with the measurement values. This confirms that the frequency response of the sensor can be calculated from the equivalent circuit shown in Fig. 2 and that the sensitivity increase at 750 MHz is caused by the increase in the effective length and the resonance of the lead wire inductance.

The relation between the sensor output level and the sensor element length was measured in a semi-anechoic chamber. A sensor was set 10 m away from the transmitting antenna, the electric field was generated by a signal generator with a power amplifier and a transmitting antenna, and the polarization of both the transmitting antenna and the sensor were set to vertical. The measurement results are shown in Fig. 7, where the solid line represents the values calculated using the equivalent circuit in Fig. 2, and the dots indicate measured values. The measured value almost agree with the calculated values, and the output voltage of the sensor is proportional to the dipole element length. This means that the equivalent circuit in Fig. 2 is useful for explaining the properties of the sensor.

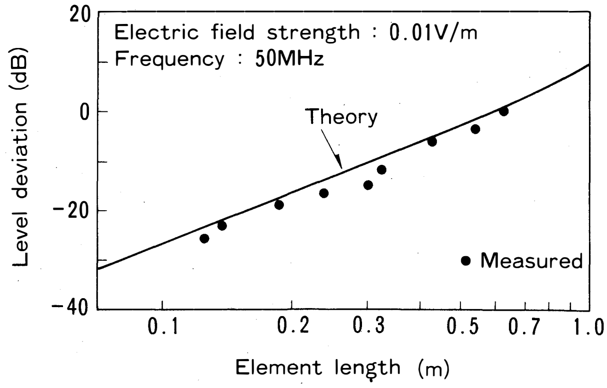

Fig. 7. Sensitivity dependence on dipole element length of the sensor.

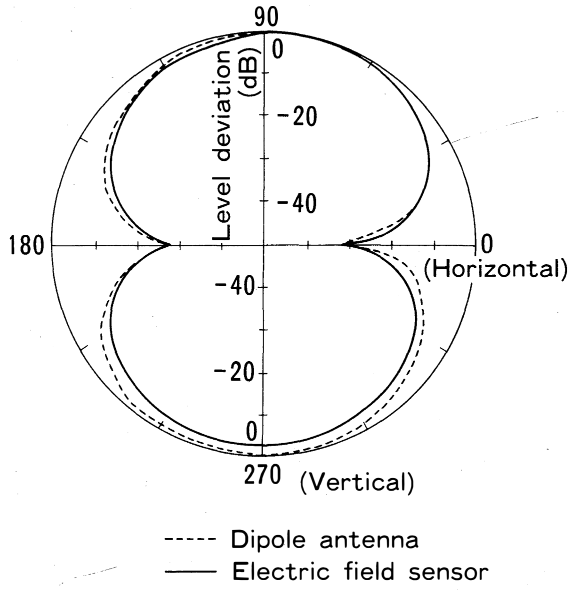

Fig. 8. Cross-polarization of the sensor.

The cross-polarization characteristics of the sensor were measured in a semi-anechoic chamber. The sensor was set on the antenna tower 10 m away from transmitting antenna, and the polarization of the sensor was tuned from 0° to 360°. The level deviation was then measure. The measurement results at 100 MHz are shown in Fig. 8. The cross-polarization of a half-wavelength dipole antenna was also measured for reference. Fig. 8 shows that the cross-polarization of the sensor is almost the same as that of the half-wavelength dipole antenna. This means that such properties of the sensor as cross polarization and directivity can be estimated by using the dipole antenna theory.

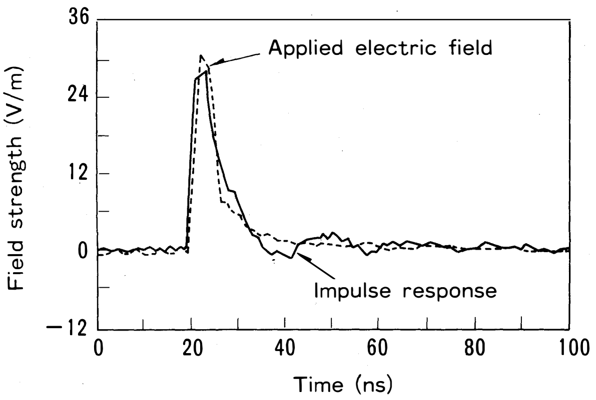

Fig. 9. Impulse response of the sensor.

VI. Impulse Response

The impulse response of the sensor was measured by using a 900 mm by 300 mm by 300 mm TEM cell, whose bandwidth is tuned to 800 MHz by absorbers. A pulse generator was connected to the input terminal of the TEM cell, and an impulse electromagnetic field was generated in the TEM cell. The waveform of the pulse was estimated from the waveform measured at the output terminal of the TEM cell. The waveform measured by the sensor was calculated from the waveform at the photodetector and the transfer coefficient A_f derived from the data in Fig. 4. A digitizing oscilloscope was used to measure the impulse waveform.

The results are shown in Fig. 9, where the dotted line represents the applied electromagnetic pulse and the solid line represents the measured values. An electromagnetic impulse with a width of 5 ns and a peak value of about 30 V/m was generated in the TEM cell. From Fig. 9, the measured waveform agrees closely with the applied waveform. This result means that an electromagnetic impulse whose width is wider than 5 ns and whose peak value is larger than 10 V/m can be measured by this sensor.

VII. Conclusion

A sensor using electrooptical crystal has been developed to support EMC studies such as the measurement of electromagnetic pulses and the testing of EMC measurement facilities.

The sensor sensitivity is improved by using a low driving-power optical modulator with a half-wave voltage of about 4 V, and by using a high power optical source consisting of a YAG laser pumped by a laser diode. The sensor operates at a wavelength of 1.3 μm, for which many optical components are being developed because this wavelength is typical for telecommunication systems.

The sensor detected the minimum field strength of 0.22 mV/m at 50 MHz and of 0.079 mV/m at 750 MHz. The frequency response of the sensor and the sensor element length dependence were calculated theoretically by considering the inductance due to the lead wire, and the calculated value agreed closely with the measured values. This sensor can measure an electromagnetic impulse whose width is wider than 5 ns and whose peak value is larger than 10 V/m.

This sensor has sufficient performance for use in EMC measurements. Future work will check the reproducibility and precision of measurements, and will improve the temperature stability of the optical bias.

Acknowledgment

The authors would like to thank Dr. K. Asatani, Dr. M. Tokuda, and Mr. T. Nozawa for their helpful guidance. They would also like to thank Mr. M. Yanagibashi for his technical assistance.

References

[1] M. Kanda and F. X. Ries, "A broad-band isotropic real-time electric-field sensor using resistivity loaded dipole," *IEEE Trans. Electromagn. Compat.*, vol. EMC-23, no. 3, pp. 122–132, Aug. 1981.

[2] H. B. Berger, V. Kumara, and K. Matloubi, "A broadband E-field sensing system," in *Proc. 1988 IEEE Symp. Electromagn. Compat.* (Seattle, WA), Aug. 1988, pp. 383–389.

[3] K. Murakawa, N. Kuwabara, and F. Amemiya, "Radiation properties of a spherical dipole antenna," in *Proc. 1989 IEEE Symp. Electromagn. Compat.* (Nagoya), Sept. 1989, pp. 572–580.

[4] M. L. Crawford and J. L. Workman, "Spherical dipole for radiating standard fields," *Digest, 1980 Conf. Precision Electromagn. Measurements,* June 1980.

[5] R. J. Phelan, Jr., D. R. Larson, and P. A. Simpson, "A sensitive, high frequency, electromagnetic field probe using a semiconductor laser in a small loop antenna," in *Fiber Optic and Laser Sensors, III, Proc, SPIE,* vol. 566, pp. 300–306, 1986.

[6] W. R Pfaff, K. Feser, and M. Lutz, "Potential-free special sensor for fieldstrength measurement in NEMP research and testing," in *Proc. 8th International Zurich Symp. Electromagn. Compat.,* Mar. 1989, pp. 35–40.

[7] N. Kuwabara, F. Amemiya, and M. Tokuda; "An electric-field probe using a bulk $LiNbO_3$ electro-optic crystal," OEC'90, 12B3-14, Japan, 1990.

[8] K. D. Masterson, L. D. Driver, and M. Kanda, "Photonic probes for the measurement of electro-magnetic fields over broad bandwidth," *National Symp. on Electromagn. Compat.,* pp. 1–6 (Denver), 1989.

[9] J. C. Wyss and S. T. Sheeran, "A practical optical modulator and link for antenna," *J. Lightwave Technol.,* vol. LT-3, no. 2, pp. 316–321, 1984.

[10] V. B. Baglikov, R. Yu. Dolinin, E. M. Pelekhatyi, and R. F. Tavlykaev, "Investigation of an electric field sensor based on an integrated optical Mach–Zehnder modulator," *Sov. J. Quantum Electron.,* vol. 18, no. 10, pp. 1353–1355, Oct. 1988.

[11] C. H. Bulmer and S. C. Hiser, "Linear Ti:$LiNbO_3$ Modulatores at 1.3 μm for electromagnetic field sensing," *Integrated Optical Circuit Eng., SPIE,* vol. 517, pp. 177–185, 1984.

[12] J. D. Kraus, Antennas. New York: McGraw Hill, 1950.

[13] K. Kawano, T. Kitoh, O. Mitomi, T. Nozawa, and H. Jumonji, "A wide-band and low-driving power phase modulator employing a Ti:$LiNbO_3$ optical waveguide at 1.5 μm wavelength," *IEEE Photon. Technol., Lett.,* vol. 1, no. 2, Feb. 1989.

[14] R. F. Harrinton, *Field Computation by Moment Method.* New York: Macmillan, 1968.

[15] W. L. Stutzman, *Antenna Theory and Design.* New York: Wiley, 1981, ch. 7.

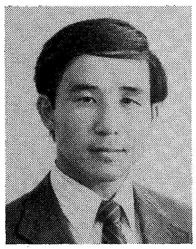

Nobuo Kuwabara (S'73–M'77) was born in Gifu, Japan on June 1, 1952. He received the B.E. and the M.E. degrees in electrical engineering from Shizuoka University, Shizuoka, Japan, in 1974 and 1976 respectively, and the Ph.D. degrees from Shizuoka University in 1992.

He is currently a Senior Research Engineer in the electromagnetic compatibility group of Telecommunication Networks Laboratories, NTT. Since joining NTT in 1977, he has been engaged in research on the overvoltage protection of telecommunications equipment, and design of optical fiber cables. He is currently involved in studies of the electromagnetic compatibility on telecommunications system.

Dr. Kuwabara is a member of the IEICE in Japan.

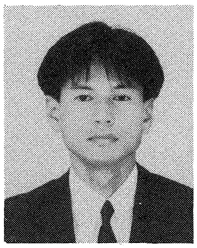

Kimihiro Tajima was born in Fukuoka, Japan, on August 3, 1962 He received the B.E and M.E. degrees in electronic engineering from Kumamoto University, Kumamoto, Japan, in 1986 and 1989, respectively.

He joined the Telecommunication Networks Laboratories of Nippon Telegraph and Telephone Corporation (NTT) in 1989. He was engaged in the studies on the optical measuring methods for Electromagnetic Compatibility. He has been in EMC Project of NTT Technical Assistance & Support Center (TASC) since 1991, and supports field engineers technically in the case of EMC troubles.

Mr. Tajima is a member of the Institute of Electronics, Information and Communication Engineers (IEICE), Japan.

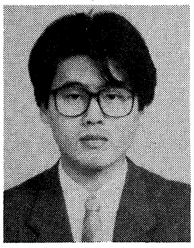

Ryuichi Kobayashi was born in Miyazaki, Japan, on January 14, 1969. He received the B.E.E. degree from the University of Electro-Communications, Chofu-shi, Tokyo, Japan, in 1991. He is continuously studying toward the M.E.E. degree in the University of Electro-Communications. His research interests are in the area of electric field measurement applying optical technology.

Mr. Kobayashi is an associated member of the IEICE in Japan.

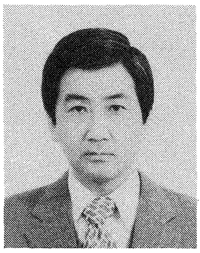

Fujio Amemiya was born in Yamanashi, Japan on February 19, 1949. He received the B.E. and M.E. degrees in electrical and communication engineering from Tohoku Univeristy, Sendai, Japan, in 1974 and 1973, respectively.

He is currently a Senior Research Engineer, Supervisor in the electromagnetic compatibility group of Telecommunication Networks Laboratories, NTT. Since joining NTT in 1973, he has been engaged in developmental research on electronic and digital telephone sets. From 1988 he has been engaged in research and development of electromagnetic compatibility on telecommunications systems.